ELSEVIER

Contents lists available at ScienceDirect

Analytica Chimica Acta

journal homepage: www.elsevier.com/locate/aca



RNA sampling from tissue sections using infrared laser ablation



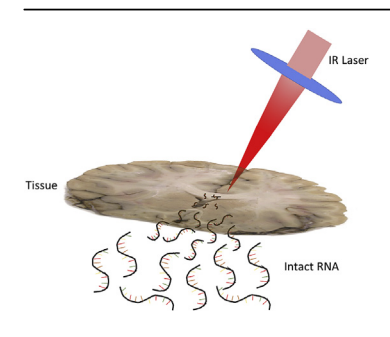
Kelin Wang ^a, Fabrizio Donnarumma ^a, Scott W. Herke ^b, Chao Dong ^a, Patrick F. Herke ^b, Kermit K. Murray ^{a, *}

- ^a Department of Chemistry, Louisiana State University, Baton Rouge, LA, 70803, United States
- ^b Genomics Facility, College of Science, Louisiana State University, Baton Rouge, LA, 70803, United States

HIGHLIGHTS

- Localized RNA microsampling from tissue using IR laser ablation capture.
- RNA sampling efficiency 75%.
- RNA integrity >90% after laser ablation.
- Captured RNA used for cDNA synthesis and mRNA quantification.

G R A P H I C A L A B S T R A C T



ARTICLE INFO

Article history: Received 17 December 2018 Received in revised form 17 February 2019 Accepted 24 February 2019 Available online 7 March 2019

Keywords: Laser ablation RNA Extraction Rat brain tissue Bioanalyzer qPCR

ABSTRACT

RNA was obtained from discrete locations of frozen rat brain tissue sections through infrared (IR) laser ablation using a 3- μ m wavelength in transmission geometry. The ablated plume was captured in a microcentrifuge tube containing RNAse-free buffer and processed using a commercial RNA purification kit. RNA transfer efficiency and integrity were evaluated based on automated electrophoresis in microfluidic chips. Reproducible IR-laser ablation of intact RNA was demonstrated with purified RNA at laser fluences of 3–5 kJ/m² (72 \pm 12% transfer efficiency) and with tissue sections at a laser fluence of 13 kJ/m² (79 \pm 14% transfer efficiency); laser energies were attenuated ~20% by the soda-lime glass slides used to support the samples. RNA integrity from tissue ablation was >90% of its original RIN value (~7) and the purified RNA was sufficiently intact for conversion to cDNA and subsequent qPCR assay.

© 2019 Elsevier B.V. All rights reserved.

1. Introduction

Ribonucleic acid (RNA) is the link between the transcription of DNA and the expression of proteins [1,2], and can reveal or modify biological function throughout the protein synthesis process [3,4].

E-mail address: kkmurray@lsu.edu (K.K. Murray).

As such, RNA biomarkers can be used for detection of a disease even before expression of the associated proteins. Further, RNA-based therapeutics can alter the production of aberrantly expressed proteins. With the increasing availability of high-throughput RNA analysis techniques such as quantitative polymerase chain reaction (qPCR) [5,6], microarray assays [7], and next generation sequencing [8–11], analyzing RNA extracted from tissue is becoming more valuable in disease diagnosis, prognosis, and drug development [12–15].

Analyte extraction and purification influences both the quantity

^{*} Corresponding author. 331 Choppin Hall, Department of Chemistry, Louisiana State University, LA, 70803, United States.

and the integrity of RNA and plays a critical role in the accuracy and reproducibility of high throughput RNA analysis [16–24]. Isolation and purification of RNA generally starts with tissue homogenization and cell lysis. For instance, tissue samples may be snap-frozen, pulverized into powder, and extracted with guanidinium thiocyanate and phenol-chloroform mixtures [25,26]. Alternatively, fresh or frozen tissue may be immersed in an RNA-stabilizing buffer and homogenized by vortexing or bead-beating [27,28]. The RNA can then be purified using a wide variety of in-house developed protocols or commercial RNA extraction kits [29–35].

Frozen or formalin-fixed paraffin embedded (FFPE) tissue is a common clinical sample type, and it is often critical to obtain RNA from a particular region of cells within a block. In this context, analysis of RNA presents challenges in maintaining analyte integrity as well as spatial localization [36]. First, the sampling method must overcome the usual obstacles to the extraction of high-quality RNA such as tissue types recalcitrant to homogenization or rich in co-purifying biomolecules (lipids, proteins, DNA) as well as degradation by ribonucleases (RNase) [29,30,37,38]. RNases are of particular concern because they can rapidly digest the RNA and are ubiquitous in tissue and the environment; therefore, fast sample processing and an RNase-free work area are critical [23,24,39]. Second, the sampling method must permit analysis of multiple RNA targets from a limited number of cells in the specific region of interest [36,40]. To date, most sampling methods cannot fully resolve these issues simultaneously. For instance, nuclease-integrity can be ensured by immediately immersing an entire tissue section in an RNA-stabilizing buffer and then homogenizing the tissue by beadbeating, but this merges the transcriptomes from all cells in the section [24]. Alternatively, single cell technologies can prevent the merging of transcriptomes, but each cell's original location within the tissue section is unknown [40–43]. Finally, techniques such as in situ hybridization [44] and in situ sequencing [45] can sample specific cells, but are limited in the number of RNA targets that can be assessed at one time [36,44].

Laser capture microdissection (LCM) is an established method for excising localized regions of interest (ROI) from tissue sections for RNA extraction from as little as a few cells [46,47]. With infrared LCM, the laser melts a thermoplastic film in contact with the tissue, causing it to stick to the film and allowing separation of the ROI from the remaining tissue [48]. With ultraviolet LCM, the laser ablates the border of the ROI and the tissue is detached from the slide with a defocused pulse [48]. The dissected material can be captured in a microcentrifuge tube and stabilized either by cooling in dry ice or by using a stabilizing RNA buffer [48–51]. Sampling time for LCM varies from 20 min to 1 h, depending on number of cells, tissue type, and type of microscope slide employed [46,52–54].

Infrared (IR) laser ablation can be used to excise ROI from tissue sections with direct collection in an appropriate biomolecule-stabilizing buffer. IR lasers operating at a $3-\mu m$ wavelength ablate tissue efficiently due to the overlap with the OH-stretch of abundant biomolecules (e.g., H_2O) [55–57], and the method has been used to sample tissues for large biomolecules such as proteins [52,58,59], biologically active enzymes [57,60], and DNA [61]. Several characteristics of IR laser ablation may be particularly useful for RNA analysis of clinical samples: disruption of connective tissue and membranes permits RNA purification without a separate cell lysis step [52,60,61]; and, 1 mm² regions can be sampled in under 60 s [52]. Thus, IR laser ablation combines sample localization with rapid sampling of the ROI.

In this work, IR laser ablation and capture was used to collect RNA from tissue. Thin fresh-frozen tissue sections of rat brain were ablated at various laser fluences, and the RNA integrity, total RNA recovery, and sample transfer efficiency for the collected material

were determined. Finally, RNA obtained by IR laser ablation was analyzed with a simple qPCR assay.

2. Experimental

2.1. Reagents and samples

Reagent suppliers were as follows (see Table S1 for a complete listing): Zymo Research (Irvine, CA) for RNA sample preservation and extraction reagents; Agilent Technologies (Santa Clara, CA) for Bioanalyzer reagents; Sakura Finetek (Torrance, CA) for tissue mounting solution; and, ThermoFisher Scientific (Waltham, MA) for all other reagents. Brain tissue samples were obtained from 4month-old breeding rats at the LSU School of Veterinary Medicine Division of Laboratory Animal Medicine in accordance with the requirements of the LSU Institutional Animal Care and Use Committee. Rats were sacrificed by exposure to carbon dioxide (5 psi) and the brain was subsequently removed intact, snap-frozen in liquid nitrogen within 30 min, and stored at -80 °C before sectioning at a thickness of 50 µm. For sectioning, one side of a rat brain was fixed to the cryostat (CM1850, Leica Microsystems, Wetzlar, Germany) support using optimal cutting temperature solution, and cryostat sections were thaw-mounted on glass microscope slides at $-25\,^{\circ}$ C. Tissue sections were vacuum-dried for 3 min prior to laser ablation.

2.2. Infrared laser ablation and capture

Samples were ablated with a wavelength tunable pulsed IR optical parametric oscillator (IR Opolette, Carlsbad, CA, USA) in transmission geometry at a repetition rate of 20 Hz and 2940 nm wavelength [60,61]. The laser has a pulse width of 7 ns and was focused to a spot size of 200 \times 250 μm at 2 mJ pulse energy and was attenuated using an external element. Prepared microscope slides were mounted on a two-axis translation stage (2 x LTA-HS, Newport, Irvine, CA, USA) with the samples facing downward. The laser was focused with a 50-mm focal length lens and directed through the microscope slide at a 45° angle. The soda—lime glass slides had ~80% transmission at the ablation laser wavelength. Visualization of samples was achieved with a CMOS camera (DCC1645C, Thorlabs, Newton, NJ). Samples were ablated into 200 µl capture buffer in a nuclease-free PCR tube mounted 5 mm below the ablation spot [52]. Custom Lab-VIEW software was used to control the laser, translation stages, and camera, allowing ablation of selected ROI in a raster pattern at 1 mm/s. Raster lines overlapped by ~50% and were separated by approximately half the 200 µm laser spot diameter.

For ablation of purified RNA, 1 μ l (1 μ g/ μ l) of human kidney total RNA was deposited on a microscope slide and vacuum-dried (1 min) prior to laser ablation. The ablated material was captured in RNA storage solution (1 mM sodium citrate, pH 6.4 \pm 0.2, ThermoFisher), and the samples were stored at $-80\,^{\circ}$ C prior to analysis. For tissue sections, the ablated material was captured in DNA/RNA Shield solution which, according to the manufacturer (Zymo Research), stabilizes nucleic acids for up to 30 days at 4 $^{\circ}$ C - 25 $^{\circ}$ C. Samples were stored at room temperature (~20 $^{\circ}$ C) up to one week until further analysis.

2.3. RNA purification

Human kidney RNA samples were loaded on the Bioanalyzer chip with no further purification. The tissue samples (ablated and positive control) were first purified using the Direct-zol RNA MicroPrep kit. The purification procedure was modified (see supporting information) to minimize salt-carryover into the eluted

sample. Without these modifications, the final salt concentration exceeded the maximum recommended for the RNA 6000 Pico kit due to the high volume of wash buffer required to process the large sample volume.

Briefly, the ablated tissue was captured in 200 ul of DNA/RNA Shield solution and transferred to a 0.5-ml tube for digestion with Proteinase K (30 min, 55 °C). Following centrifugation to pellet cellular debris, the cleared supernatant was transferred to a 2.0-ml tube containing ~800 µl of TRI-reagent and rotated in a 30 °C oven (5 min). Following the addition of 1 mL of 100% ethanol, the tube was briefly rotated in the oven to ensure thorough mixing. For each sample, a spin-column (Zymo IC, designed for low elution volumes) was loaded and centrifuged three times to filter the entire 2000 µl of RNA extraction reagents. Unless otherwise noted, centrifugation was performed at 15,000 rcf and limited to 15 s to prevent column drying, which can increase the salt in the final elution. Following the application of RNA wash buffer (400 µl, 30 s), an in-column DNAse I digestion was performed (30 °C, 15 min). After two applications of pre-wash buffer (400 µl), RNA wash buffer was applied three times (350 μ l, 700 μ l, and 350 μ l) to completely remove salt from each sample. After discarding the final flow-through, the column was centrifuged for 60 s to fully remove the RNA wash buffer. Finally, RNA was eluted in 15 µl nuclease-free water (60 s, 10,000 rcf) and stored at -80 °C.

Positive controls were generated by directly placing a frozen rat brain tissue section (~1 mg) into $200\,\mu$ l of DNA/RNA Shield solution. These samples were initially homogenized by brief vortexing and then completely homogenized in ZR Bashing-Bead lysis tubes. Following centrifugation, the supernatants were transferred to 0.5 mL tubes and processed with the same workflow as the ablated samples.

2.4. RNA analysis

For choosing the optimal capture buffer, the RNA integrity was assessed by comparing the relative height for the peaks associated with ribosomal subunits 18S and 28S in control vs. laser ablated samples. However, the 28S:18S peak ratio can be a highly variable metric [62,63]; thus, RNA concentration and integrity for all other experiments were assessed using an Agilent Bioanalyzer 2100 with an RNA 6000 Pico Kit. This system uses microfluidic chip-based electrophoresis to separate RNA samples by molecular weight and quantify the RNA with respect to a standard RNA ladder run concurrently on the chip. In this assay, a typical trace displays the fluorescence intensity of the eluting components, with the lower marker eluting first (~22 s), followed by smaller RNA fragments collectively labeled as the 5S region (~24-28s) and finally the peaks for the 18S (~40s) and 28S subunits (~48s). Further, the software assesses multiple regions from the electrophoretic trace to determine an RNA integrity number (RIN). RIN values can range from 1 to 10, with 1 indicating highly degraded RNA and 10 representing fully intact RNA [63].

2.5. cDNA synthesis and qPCR quantification

Captured and purified RNA was reverse transcribed into cDNA. Samples were analyzed in triplicate by qPCR on a real-time PCR system (QuantStudio 6 Flex, Applied Biosystems) using 22-µl reaction volumes: $10\,\mu$ l of 1X SYBR Select Master Mix; $1\,\mu$ L each forward and reverse primer ($10\,\mu$ M, Table S2); and, $10\,\mu$ l of cDNA template. Cycling parameters were: 1 cycle at $50\,^{\circ}$ C ($20\,^{\circ}$ C min); 1 cycle at $95\,^{\circ}$ C ($10\,^{\circ}$ C min); and, $40\,^{\circ}$ C amplification cycles of $95\,^{\circ}$ C ($15\,^{\circ}$ C) and $10\,^{\circ}$ C ($10\,^{\circ}$ C). The specificity of the amplified product was assessed by a melt curve analysis.

3. Results

Initial experiments were performed to determine whether RNA could be captured intact using IR laser ablation and to quantify the ablation and capture efficiency. To assess RNA integrity, a commercially-purified stock of RNA (isolated from human kidney) was ablated at laser fluences ranging from 3 to $11 \, \text{kJ/m}^2$. For the positive control, a $1 \, \mu l$ aliquot of the RNA was added to $200 \, \mu l$ of RNA storage solution. Bioanalyzer data for the ablated and control RNA samples were compared with regard to their RNA integrity number (RIN) and their electrophoretic traces. Representative electropherograms are shown in Fig. 1 (triplicate electropherograms are shown in Fig. S1).

Initially, a tris-EDTA buffer (10 mM Tris, 0.05 mM EDTA, ~pH 8) was used as the capture buffer; however, the 28S peaks were consistently smaller than the 18S peaks when these samples were processed on the Bioanalyzer. By contrast, ablated samples captured in RNA storage solution typically displayed 28S peaks of equal or greater intensity than the 18S peaks, indicating that this buffer promotes greater RNA stability than does the tris-EDTA buffer.

The measured RIN values were comparable between the positive control (RIN 8.8 ± 0.4) and purified RNA ablated at low fluences $(3 \text{ kJ/m}^2, \text{RIN } 8.6 \pm 0.2; \text{ and, } 5 \text{ kJ/m}^2, \text{RIN } 8.1 \pm 0.2)$. Further, based on a two-tailed T-test, the differences between controls and ablated samples were not statistically significant at either 3 kJ/m² (p-Value = 0.471) or at 5 kJ/m^2 (p-Value = 0.053). The difference between control and sample ablated at 5 kJ/m² was near the limit of statistical significance but vielded high quality RNA. By contrast. RIN values were ~30% lower for purified RNA samples ablated at 7 and 9 kJ/m^2 (RIN 6.8 ± 0.1 and 6.3 ± 0.4 , respectively). At 11 kJ/m^2 , fluorescence readings from the small RNA region of the electropherogram were extremely high, resulting in a RIN estimate of "N/ A" (not available). Manually increasing the threshold value [63,64] for the "5S Region Anomaly Threshold" from 0.5 (default setting) to 0.62 resulted in a RIN of 4.5 ± 0.4 , which was ~50% lower than RIN for the positive control.

To summarize, with purified RNA, laser fluences of \leq 5 kJ/m² generated RIN values and electropherograms similar to those of the positive control sample. By contrast, corresponding data for RNA obtained at laser fluence \geq 7 kJ/m² demonstrated that higher laser fluences caused degradation (i.e. fragmentation) of the purified RNA, although the RIN estimates (>5) indicated that the RNA could still be used for qPCR [65,66]. As such, RNA appears to be more sensitive to IR laser ablation than was found for DNA, where a laser fluence of 24 kJ/m² did not influence purified plasmid DNA integrity [61]. These results may reflect the greater stability of double-stranded DNA compared to single-stranded RNA [67].

As assessed with the Bioanalyzer, recovery of high-quality purified RNA was the highest at 5 kJ/m², and then progressively decreased with increasing fluences. Here, we compared fluorescence readings from the entire electrophoretic trace (full trace) with those from just the 18S and 28S subunits (Table 1). Both metrics indicated that increasing the laser fluence from 3 to 5 kJ/m² resulted in higher RNA recovery. By contrast, as the fluence increased from 7 to 11 kJ/m², RNA recovery appeared to increase by the full trace metric whereas it decreased by the 18S/28S peak metric. These results reflect the fact that, upon degradation, 18S and 28S ribosomal RNA shifts towards the 5S region (Fig. 1d, f) where the degraded fragments are retained in the calculation of total RNA.

Transfer efficiency can be defined as the ratio of the quantity of material captured to the quantity originally deposited. To assess the capture efficiency, a 1 μ g quantity of RNA in 1 μ L of sodium citrate (pH 6.8) was deposited on a microscope slide and completely ablated into 200 μ l of capture buffer. For the control, 1 μ g of RNA was

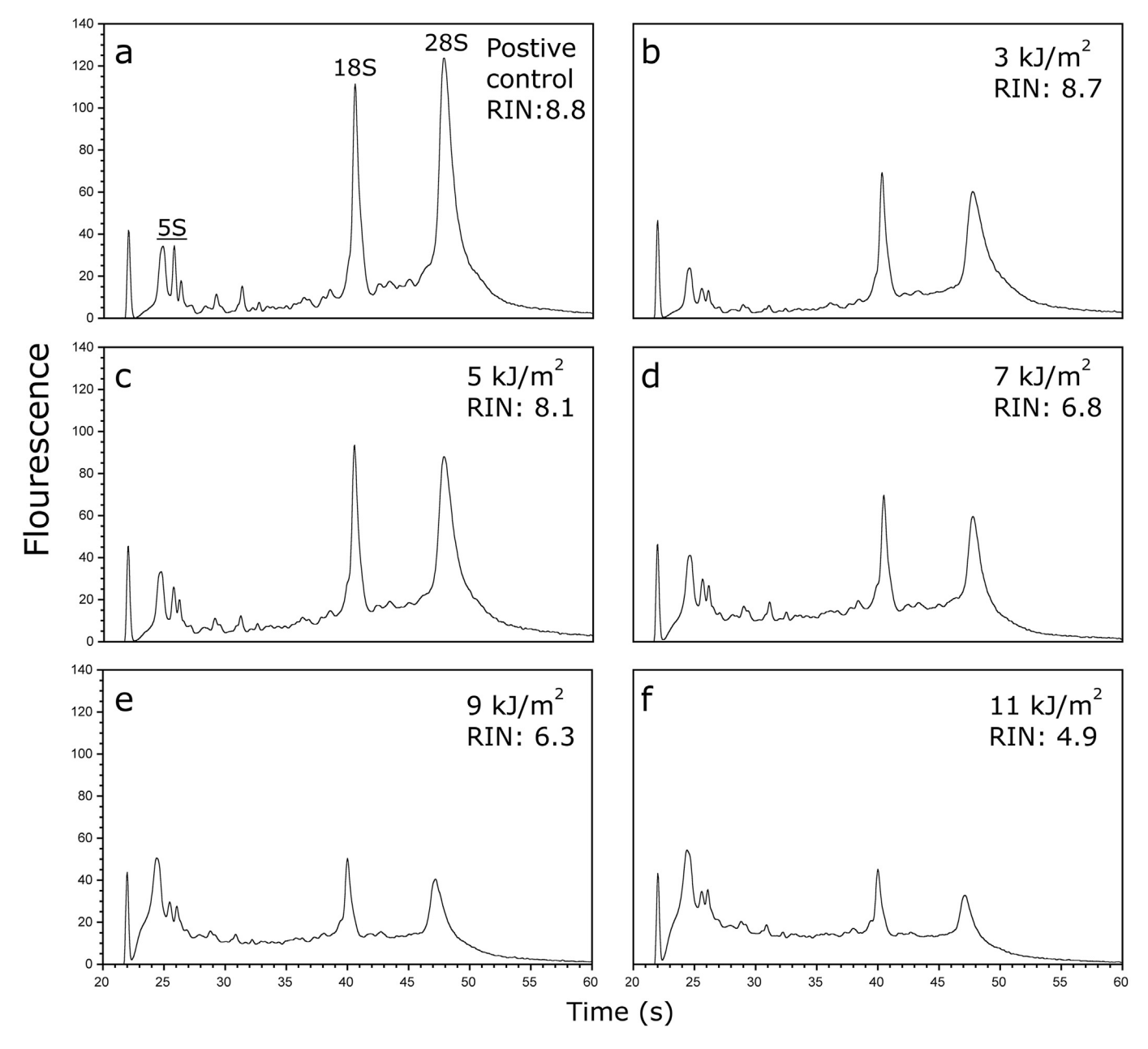


Fig. 1. Agilent Bioanalyzer electropherograms (RNA Pico 6000 kit) of purified human kidney total RNA (diluted in RNA storage solution) comparing RNA integrity number (RIN) values for a positive control (a) with RNA collected by infrared laser ablation at five different fluences (b—f: 3, 5, 7, 9, & 11 kJ/m²). At higher laser fluence, RNA is lost from the 18S and 28S peaks, with the degraded fragments contributing to baseline and the 5S region.

Table 1 RNA recovery as a function of laser fluence.

Laser Fluence (kJ/m ²)	RNA (µg), full trace	RNA (µg), 18S & 28S peaks
3	0.50 ± 0.09	0.17 ± 0.02
5	0.67 ± 0.06	0.19 ± 0.02
7	0.72 ± 0.11	0.11 ± 0.02
9	0.77 ± 0.01	0.10 ± 0.01
11	0.88 ± 0.06	0.07 ± 0.01
Positive control	0.83 ± 0.19	0.30 ± 0.02

added to 200 μ l of capture buffer. Transfer efficiency was quantified using Bioanalyzer data for samples ablated at fluences of 3 and 5 kJ/m² because they produced RIN values similar to those of controls. The average transfer efficiency for purified RNA ranged from

 $72\pm12\%$ (full trace, which includes degraded RNA) to $60\pm6\%$ (18S/28S subunits, which represent fully intact RNA). The RNA transfer efficiency determined here is similar to the IR laser ablation transfer efficiency determined for DNA (59 ±3) [61] and enzymes (75 ±8) [60].

After demonstrating that RNA can be ablated and captured intact, IR-laser ablation and capture of RNA from tissue was tested. Consecutive rat brain tissue sections were used to evaluate the quality of the total RNA after laser ablation. A rat brain was sectioned along the coronal plane at a thickness of $50\,\mu m$, and consecutive sections were thaw-mounted on microscope slides for laser ablation (samples) or placed in tubes immersed in dry ice (controls); all slides and controls were then stored at $-80\,^{\circ}$ C. For the ablation experiments, TRI-Reagent (guanidine thiocyanate and phenol) was initially used as the capture buffer; however, the 28S

peaks were consistently smaller than the 18S peaks. Ultimately, DNA/RNA Shield solution was used as the capture buffer because it maintained a more intense 28S peak (vs. the 18S peak), which indicates better preservation of RNA. Tissue sections (~20 mm² each, ~1 mg) mounted on microscope slides were ablated in their entirety using a laser fluence of $13\ kJ/m^2$; visual inspection of the slides indicated that $13\ kJ/m^2$ was the minimum laser fluence required for complete tissue ablation. Concurrently with the ablated samples, control samples were homogenized in DNA/RNA Shield solution using a bead-beating protocol (Section 2.3).

The entire volume of each ablated and control sample was purified with the Direct-zol RNA MicroPrep kit. Prior to analysis, the purified samples were diluted in nuclease-free water to bring them into the Bioanalyzer quantitation range. Control samples processed with the bead-beating method had a RIN of 7.4 ± 0.3 , whereas ablated and captured RNA had a RIN of 6.8 ± 0.3 (Fig. 2). RNA concentrations were calculated with the area under the curve method using both the full electrophoretic trace (including degraded RNA) as well as the signal for only 18S and 28S subunits (intact RNA). Transfer efficiencies ranged from $79\pm14\%$ for the full trace $(649\pm100$ ng vs. 515 ± 93 ng) to $71\pm7\%$ for the 18S-28S peaks $(245\pm8.6$ ng vs. 174 ± 18 ng).

RNA samples with RIN >5 have been analyzed with microarray assays, qPCR, and RNA sequencing [65,66,68-71]. In the results described above, RNA from ablated tissue sections had a RIN of ~7, representing only an 8% decrease compared to the conventional bead-beating method. Further, this RIN is generally consistent with values previously reported for LCM, although LCM results vary greatly depending on sampling conditions [47.49.53.72–83]. Complete ablation occurred with 3–5 kJ/m² for purified RNA; however, 13 kJ/m² was required to completely ablate rat brain tissue sections. Nevertheless, at their respective laser energies, the captured RNA for both sample types had RIN values of ~7 and the associated electropherograms were similar (Fig. 1). It is possible that the water in the tissue allows the use of higher laser energies, which are required to overcome the tensile strength of the tissue itself, without compromising the stability of the RNA molecules [84]. Preliminary experiments showed that tissue dried for more than 5 min required higher energy (>20 kJ/m²) for complete ablation and the captured RNA had lower RIN.

Finally, to augment the Bioanalyzer results, qPCR was used to assess the compatibility of laser-ablated RNA with downstream assays. Further, to demonstrate the spatial control possible with this method, RNA was laser ablated from two discrete, differently-

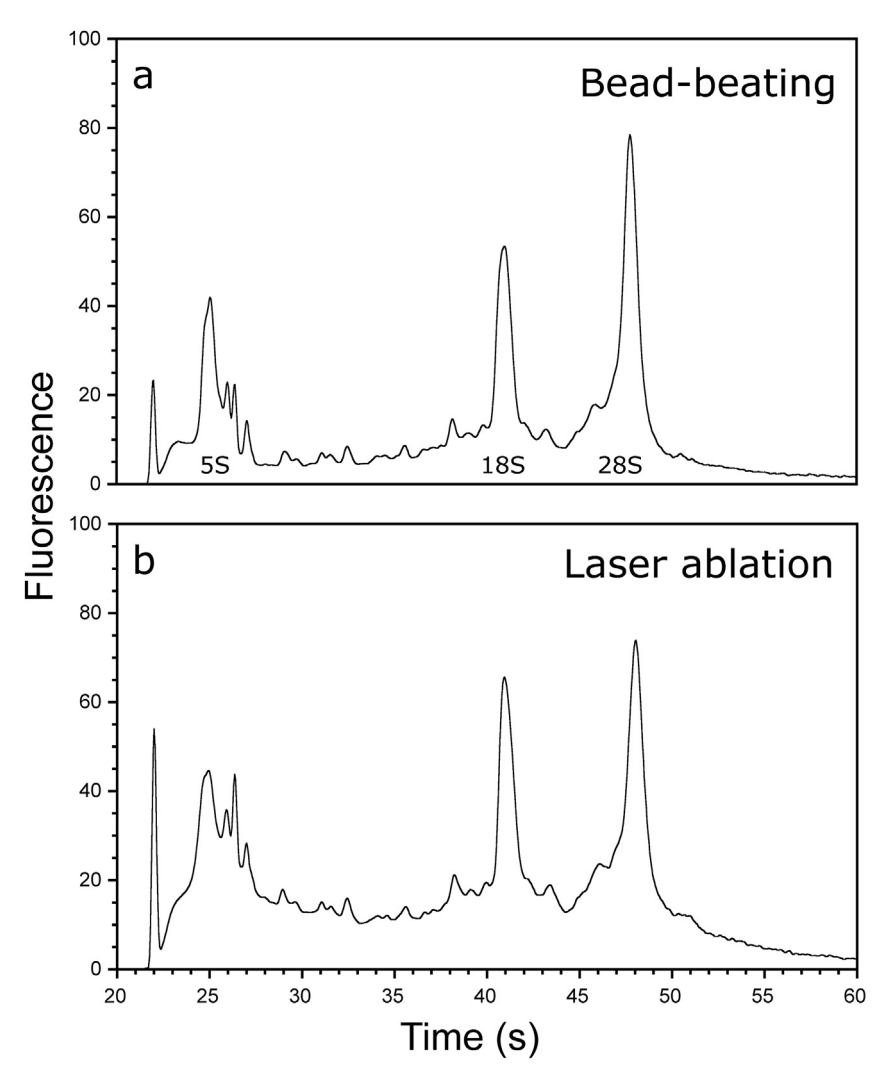


Fig. 2. Representative electropherograms of RNA from 20-mm^2 regions of paired consecutive $50 \, \mu m$ tissue sections (triplicate, see Fig. S2), showing only minor RNA degradation in the ablated sample as evidenced by the slightly reduced 28S peak and the slightly greater baseline. (a) Positive control (RIN 7.4 ± 0.3) (b) Infrared laser ablation (RIN 6.8 ± 0.3): see text for details.

shaped regions of rat brain tissue sections (Fig. 3). Location 1 comprised two 4-mm² crescents covering the corpus callosum region and location 2 comprised a 3-mm² circle in the hypothalamus region. Following purification, the ablated RNA had intense 18S/28S peaks and good overall integrity (Location 1, RIN 7.4; Location 2, RIN 7.3). For qPCR, two sets of primers targeting two different genes were used [85]. One primer was designed for the house-keeping gene *glyceraldehyde-3-phosphate dehydrogenase*. The other primer targeted *myelin basic protein* (MBP), an important protein in the process of myelination of nerves in the nervous system [86]. For both locations and both genes, the cDNA produced from the RNA generated C_t values between ~22 and 28 cycles (Fig. 3-a) and melt curves which indicated that each primer pair produced a single, specific final product (Fig. 3-b).

4. Conclusions

IR laser ablation can be used to ablate and capture intact RNA from pure samples and from tissue sections. The transfer efficiency ranged from 60 to 80% and is comparable to that observed for IR laser ablation of DNA and proteins [60,87]. For dried purified RNA

samples, a laser fluence of $5 \, kJ/m^2$ (ca. $300 \, \mu J$ energy) resulted in efficient ablation and high RNA integrity. Considerably more energy (~2.5X) was required to ablate the tissue samples for comparable RNA capture efficiency and integrity. The higher energy required for tissue is likely due to the need to disrupt the connective structures of the tissue.

The ability to sample both proteins and RNA from tissue opens up new opportunities for combined proteomics and transcriptomics. The combination of mass spectrometry-based proteomics with mRNA transcriptomics has been used to study the correlation between protein level and corresponding mRNA level [88–91], and to elucidate factors of correlation such as post-translational regulation [92,93] and gene copy number variation [94]. Future studies will combine the localized RNA ablation and capture described above with previously demonstrated infrared laser ablation and capture for proteomics [52,58] for localized proteomics/transcriptomics studies. This combined approach has the potential to provide information about gene transcription as well as protein quantification from the same region of interest.

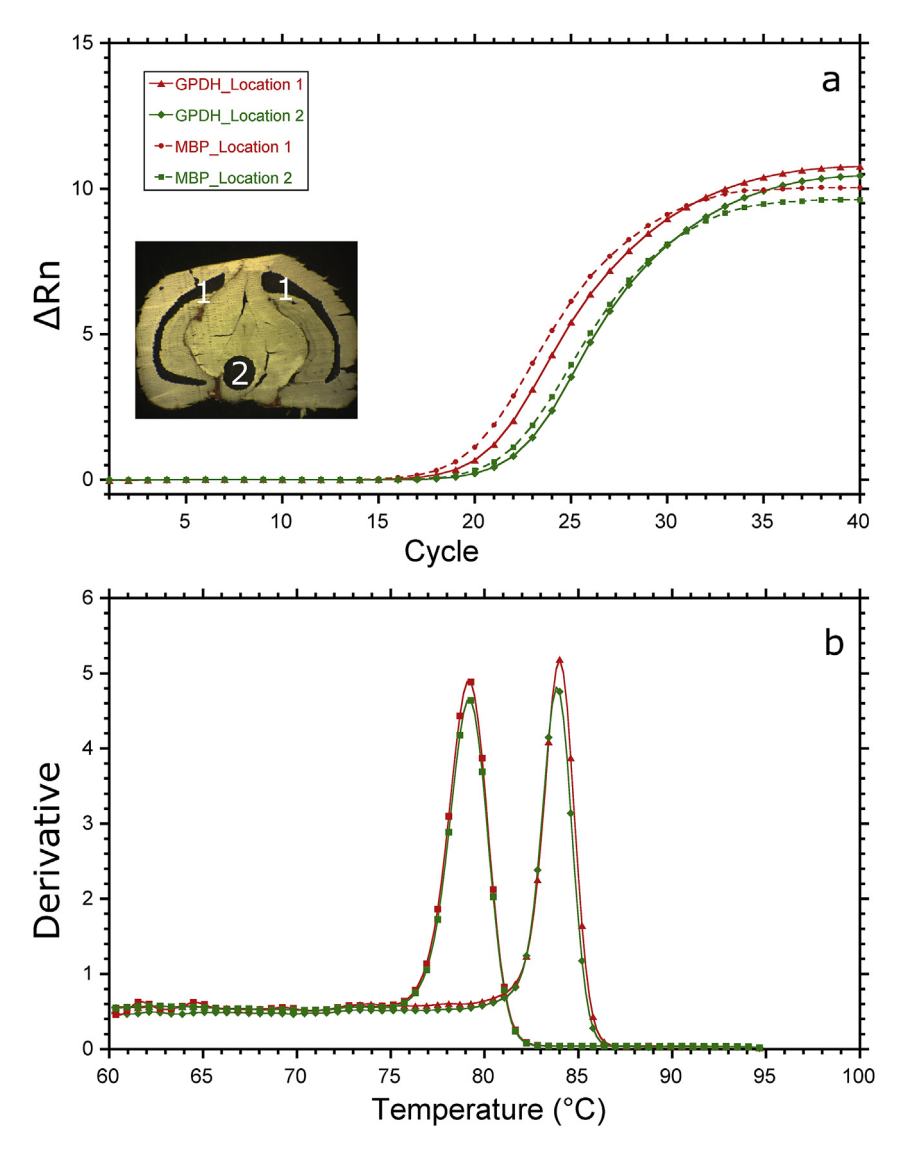


Fig. 3. Analysis by qPCR of RNA captured from two locations of a rat brain tissue section (a, insert): Location 1, corpus callosum (two 4-mm² crescents); Location 2, hypothalamus (3-mm² circle). The cDNA from both locations generated similar qPCR results (a – amplification curves; b – melt curves) for two genes (MBP; GPDH).

Conflict of interest

The authors declare that they have no conflict of interest.

Acknowledgements

This material is based upon work supported by the National Science Foundation under Grant No. DBI-1556000 and CHE-1709526. The authors thank Dr. D. G. Baker (School of Veterinary Medicine, Louisiana State University) for kindly providing rat brain samples.

Appendix A. Supplementary data

Supplementary data to this article can be found online at https://doi.org/10.1016/j.aca.2019.02.054.

References

- [1] A. Serganov, E. Nudler, A decade of riboswitches, Cell 152 (2013) 17-24.
- [2] R.R. Breaker, G.F. Joyce, The expanding view of RNA and DNA function, Chem. Biol. 21 (2014) 1059–1065.
- [3] C.M. Connelly, M.H. Moon, J.S. Schneekloth Jr., The emerging role of RNA as a therapeutic target for small molecules, Cell Chem. Biol. 23 (2016) 1077–1090.
- [4] D.H. Kim, J.J. Rossi, Strategies for silencing human disease using RNA interference, Nat. Rev. Genet. 8 (2007) 173–184.
- [5] R. Sanders, D.J. Mason, C.A. Foy, J.F. Huggett, Evaluation of digital PCR for absolute RNA quantification, PLoS One 8 (2013) e75296.
- [6] D.M. Maslove, H.R. Wong, Gene expression profiling in sepsis: timing, tissue, and translational considerations, Trends Mol. Med. 20 (2014) 204–213.
- [7] D. Chickooree, K. Zhu, V. Ram, H.J. Wu, Z.J. He, S. Zhang, A preliminary microarray assay of the mi RNA expression signatures in buccal mucosa of oral submucous fibrosis patients, J. Oral Pathol. Med. 45 (2016) 691–697.
- [8] Y. Chu, D.R. Corey, RNA sequencing: platform selection, experimental design, and data interpretation, Nucleic Acid Ther. 22 (2012) 271–274.
- [9] S.A. Byron, K.R. Van Keuren-Jensen, D.M. Engelthaler, J.D. Carpten, D.W. Craig, Translating RNA sequencing into clinical diagnostics: opportunities and challenges, Nat. Rev. Genet. 17 (2016) 257.
- [10] L. Liu, Y. Li, S. Li, N. Hu, Y. He, R. Pong, D. Lin, L. Lu, M. Law, Comparison of next-generation sequencing systems, J. Biomed. Biotechnol. 2012 (2012) 251364
- [11] F. Ozsolak, P.M. Milos, RNA sequencing: advances, challenges and opportunities, Nat. Rev. Genet. 12 (2011) 87–98.
- [12] M.L. Idda, R. Munk, K. Abdelmohsen, M. Gorospe, Noncoding RNAs in Alzheimer's disease, Wiley Interdiscip. Rev. RNA 9 (2018) e1463.
- [13] C. Teixidó, A. Giménez-Capitán, M.Á. Molina-Vila, V. Peg, N. Karachaliou, A. Rodríguez-Capote, J. Castellví, R. Rosell, RNA analysis as a tool to determine clinically relevant gene fusions and splice variants, Arch. Pathol. Lab. Med. 142 (2018) 474–479.
- [14] P. Quarello, E. Garelli, A. Carando, C. Mancini, L. Foglia, C. Botto, P. Farruggia, K. De Keersmaecker, A. Aspesi, S.R. Ellis, Ribosomal RNA analysis in the diagnosis of diamond-blackfan anaemia, Br. J. Haematol. 172 (2016) 782–785.
- [15] S. Serratì, S. De Summa, B. Pilato, D. Petriella, R. Lacalamita, S. Tommasi, R. Pinto, Next-generation sequencing: advances and applications in cancer diagnosis, OncoTargets Ther. 9 (2016) 7355–7365.
- [16] J. Vermeulen, K. De Preter, S. Lefever, J. Nuytens, F. De Vloed, S. Derveaux, J. Hellemans, F. Speleman, J. Vandesompele, Measurable impact of RNA quality on gene expression results from quantitative PCR, Nucleic Acids Res. 39 (2011) e63-e63.
- [17] S. Derveaux, J. Vandesompele, J. Hellemans, How to do successful gene expression analysis using real-time PCR, Methods 50 (2010) 227–230.
- [18] L. Opitz, G. Salinas-Riester, M. Grade, K. Jung, P. Jo, G. Emons, B.M. Ghadimi, T. Beißbarth, J. Gaedcke, Impact of RNA degradation on gene expression profiling, BMC Med. Genomics 3 (2010) 36.
- [19] S. Cepollaro, E. Della Bella, D. de Biase, M. Visani, M. Fini, Evaluation of RNA from human trabecular bone and identification of stable reference genes, J. Cell. Physiol. 233 (2018) 4401–4407.
- [20] J.M. Taylor, The isolation of eukaryotic messenger RNA, Annu. Rev. Biochem. 48 (1979) 681–717.
- [21] D.G. Walker, A.M. Whetzel, G. Serrano, L.I. Sue, L.-F. Lue, T.G. Beach, Characterization of RNA isolated from eighteen different human tissues: results from a rapid human autopsy program, Cell Tissue Bank. 17 (2016) 361–375.
- [22] I.N. Sirakov, Nucleic Acid Isolation and Downstream Applications, Nucleic Acids-From Basic Aspects to Laboratory Tools, InTech, 2016.
- [23] M. Kap, A.M. Sieuwerts, M. Kubista, M. Oomen, S. Arshad, P. Riegman, The influence of tissue procurement procedures on RNA integrity, gene expression, and morphology in porcine and human liver tissue, Biopreserv. Biobank. 13 (2015) 200–206.
- [24] Z. Salehi, M. Najafi, RNA preservation and stabilization, Biochem. Physiol. 3

- (2014) 2.
- [25] S. Cirera, Highly efficient method for isolation of total RNA from adipose tissue, BMC Res. Notes 6 (2013) 472.
- [26] S. Caprez, U. Menzel, Z. Li, S. Grad, M. Alini, M. Peroglio, Isolation of high-quality RNA from intervertebral disc tissue via pronase predigestion and tissue pulverization, JOR Spine 1 (2018) e1017.
- [27] R. Verollet, A major step towards efficient sample preparation with beadbeating, Biotechniques 44 (2008) 832–833.
- [28] G. Banneau, M. Ayadi, L. Armenoult, E. Carvalho, Homogenization of cartilage tumors to extract total RNA to microarray and sequencing analysis using Precellys bead-beating technology, Biotechniques 52 (2012) 196–197.
- [29] N. Ali, R.d.C.P. Rampazzo, A.D.T. Costa, M.A. Krieger, Current nucleic acid extraction methods and their implications to point-of-care diagnostics, Bio-Med Res. Int. (2017), 9306564.
- [30] J.M. Chirgwin, A.E. Przybyla, R.J. MacDonald, W.J. Rutter, Isolation of biologically active ribonucleic acid from sources enriched in ribonuclease, Biochemistry 18 (1979) 5294–5299.
- [31] P. Chomczynski, N. Sacchi, The single-step method of RNA isolation by acid guanidinium thiocyanate—phenol—chloroform extraction: twenty-something years on, Nat. Protoc. 1 (2006) 581–585.
- [32] P. Chomczynski, N. Sacchi, Single-step method of RNA isolation by acid guanidinium thiocyanate-phenol-chloroform extraction, Anal. Biochem. 162 (1987) 156–159.
- [33] C. Watermann, K. Peter Valerius, S. Wagner, C. Wittekindt, J. Peter Klussmann, E. Baumgart-Vogt, S. Karnati, Step-by-step protocol to perfuse and dissect the mouse parotid gland and isolation of high-quality RNA from murine and human parotid tissue. Biotechniques 60 (2016) 200–203.
- [34] M. Griffin, M. Abu-El-Haija, M. Abu-El-Haija, T. Rokhlina, A. Uc, Simplified and versatile method for isolation of high-quality RNA from pancreas, Biotechniques 52 (2012) 332–334.
- [35] P. Tesena, W. Korchunjit, J. Taylor, T. Wongtawan, Comparison of commercial RNA extraction kits and qPCR master mixes for studying gene expression in small biopsy tissue samples from the equine gastric epithelium, J. Equine Sci. 28 (2017) 135—141.
- [36] N. Crosetto, M. Bienko, A. Van Oudenaarden, Spatially resolved transcriptomics and beyond, Nat. Rev. Genet. 16 (2015) 57–66.
- [37] A.C.P. Azevedo-Pouly, O.A. Elgamal, T.D. Schmittgen, RNA isolation from mouse pancreas: a ribonuclease-rich tissue, J. Vis. Exp. (2014) e51779.
- [38] P.A. Krieg, A Laboratory Guide to RNA: Isolation, Analysis, and Synthesis, John Wiley & Sons, 1996.
- [39] R.E. Farrell Jr., RNA Methodologies: Laboratory Guide for Isolation and Characterization, Academic Press, 2009.
- [40] C. Strell, M.M. Hilscher, N. Laxman, J. Svedlund, C. Wu, C. Yokota, M. Nilsson, Placing RNA in context and space—methods for spatially resolved transcriptomics, FEBS J. (2018) 14435.
- [41] A.A. Kolodziejczyk, J.K. Kim, V. Svensson, J.C. Marioni, S.A. Teichmann, The technology and biology of single-cell RNA sequencing, Mol. Cell 58 (2015) 610–620.
- [42] Y. Hou, H. Guo, C. Cao, X. Li, B. Hu, P. Zhu, X. Wu, L. Wen, F. Tang, Y. Huang, Single-cell triple omics sequencing reveals genetic, epigenetic, and transcriptomic heterogeneity in hepatocellular carcinomas, Cell Res. 26 (2016) 304–319.
- [43] A.E. Moor, S. Itzkovitz, Spatial transcriptomics: paving the way for tissue-level systems biology, Curr. Opin. Biotechnol. 46 (2017) 126–133.
- [44] C. Cui, W. Shu, P. Li, Fluorescence in situ hybridization: cell-based genetic diagnostic and research applications, Front. Cell Dev. Biol. 4 (2016) 89.
- [45] T. Nawy, In situ sequencing, Nat. Methods 11 (2013) 29.
- [46] S. Datta, L. Malhotra, R. Dickerson, S. Chaffee, C.K. Sen, S. Roy, Laser capture microdissection: big data from small samples, Histol. Histopathol. 30 (2015) 1255–1269.
- [47] S. Farris, Y. Wang, J.M. Ward, S.M. Dudek, Optimized method for robust transcriptome profiling of minute tissues using laser capture microdissection and low-input RNA-Seq, Front. Mol. Neurosci. 10 (2017) 185.
- [48] M. Vandewoestyne, K. Goossens, C. Burvenich, A. Van Soom, L. Peelman, D. Deforce, Laser capture microdissection: should an ultraviolet or infrared laser be used? Anal. Biochem. 439 (2013) 88–98.
- [49] K. Kolijn, G.J. Leenders, Comparison of RNA extraction kits and histological stains for laser capture microdissected prostate tissue, BMC Res. Notes 9 (2016) 17.
- [50] G. Lugli, Y. Kataria, Z. Richards, P. Gann, X. Zhou, L. Nonn, Laser-capture microdissection of human prostatic epithelium for RNA analysis, J. Vis. Exp. (2015) e53405.
- [51] W.-Z. Wang, F.M. Oeschger, S. Lee, Z. Molnár, High quality RNA from multiple brain regions simultaneously acquired by laser capture microdissection, BMC Mol. Biol. 10 (2009) 69.
- [52] F. Donnarumma, K.K. Murray, Laser ablation sample transfer for localized LC-MS/MS proteomic analysis of tissue, J. Mass Spectrom. 51 (2016) 261–268.
- [53] U. Rudloff, U. Bhanot, W. Gerald, D.S. Klimstra, W.R. Jarnagin, M.F. Brennan, P.J. Allen, Biobanking of human pancreas cancer tissue: impact of ex-vivo procurement times on RNA quality, Ann. Surg. Oncol. 17 (2010) 2229–2236.
- [54] D.M. Kube, C.D. Savci-Heijink, A.-F. Lamblin, F. Kosari, G. Vasmatzis, J.C. Cheville, D.P. Connelly, G.G. Klee, Optimization of laser capture microdissection and RNA amplification for gene expression profiling of prostate cancer, BMC Mol. Biol. 8 (2007) 25.
- [55] S.-G. Park, K.K. Murray, Infrared laser ablation sample transfer for MALDI

- imaging, Anal. Chem. 84 (2012) 3240-3245.
- [56] S.-G. Park, K.K. Murray, Infrared laser ablation sample transfer for MALDI and electrospray, J. Am. Soc. Mass Spectrom. 22 (2011) 1352–1362.
- [57] M. Kwiatkowski, M. Wurlitzer, M. Omidi, L. Ren, S. Kruber, R. Nimer, W.D. Robertson, A. Horst, R.D. Miller, H. Schlüter, Ultrafast extraction of proteins from tissues using desorption by impulsive vibrational excitation, Angew. Chem. Int. Ed. 54 (2015) 285–288.
- [58] F. Donnarumma, F. Cao, K.K. Murray, Laser ablation with vacuum capture for MALDI mass spectrometry of tissue, J. Am. Soc. Mass Spectrom. 27 (2016) 108–116.
- [59] L. Ren, W.D. Robertson, R. Reimer, C. Heinze, C. Schneider, D. Eggert, P. Truschow, N.-O. Hansen, P. Kroetz, J. Zou, Towards instantaneous cellular level bio diagnosis: laser extraction and imaging of biological entities with conserved integrity and activity, Nanotechnology 26 (2015) 284001.
- [60] K. Wang, F. Donnarumma, M.D. Baldone, K.K. Murray, Infrared laser ablation and capture of enzymes with conserved activity, Anal. Chim. Acta (2018) 41–46.
- [61] K. Wang, F. Donnarumma, S.W. Herke, P.F. Herke, K.K. Murray, Infrared laser ablation sample transfer of tissue DNA for genomic analysis, Anal. Bioanal. Chem. 409 (2017) 4119—4126.
- [62] V. Copois, F. Bibeau, C. Bascoul-Mollevi, N. Salvetat, P. Chalbos, C. Bareil, L. Candeil, C. Fraslon, E. Conseiller, V. Granci, Impact of RNA degradation on gene expression profiles: assessment of different methods to reliably determine RNA quality, J. Biotechnol. 127 (2007) 549–559.
- [63] A. Schroeder, O. Mueller, S. Stocker, R. Salowsky, M. Leiber, M. Gassmann, S. Lightfoot, W. Menzel, M. Granzow, T. Ragg, The RIN: an RNA integrity number for assigning integrity values to RNA measurements, BMC Mol. Biol. 7 (2006) 3.
- [64] M. Terada, M. Seki, A. Higashibata, S. Yamada, R. Takahashi, H.J. Majima, T. Yamazaki, T. Watanabe-Asaka, M. Niihori, C. Mukai, Genetic analysis of the human hair roots as a tool for spaceflight experiments, Adv. Biosci. Biotechnol. 4 (2013) 75–88.
- [65] S. Fleige, M.W. Pfaffl, RNA integrity and the effect on the real-time qRT-PCR performance, Mol. Aspect. Med. 27 (2006) 126–139.
- [66] C. Strand, J. Enell, I. Hedenfalk, M. Fernö, RNA quality in frozen breast cancer samples and the influence on gene expression analysis—a comparison of three evaluation methods using microcapillary electrophoresis traces, BMC Mol. Biol. 8 (2007) 38.
- [67] T. Lindahl, The intrinsic fragility of DNA (Nobel Lecture), Angew. Chem. Int. Ed. 55 (2016) 8528–8534.
- [68] C. Becker, A. Hammerle-Fickinger, I. Riedmaier, M. Pfaffl, mRNA and microRNA quality control for RT-qPCR analysis, Methods 50 (2010) 237–243.
- [69] K.R. Kukurba, S.B. Montgomery, RNA sequencing and analysis, Cold Spring Harb. Protoc. (2015) 951–969.
- [70] S. Weis, I. Llenos, J. Dulay, M. Elashoff, F. Martinez-Murillo, C. Miller, Quality control for microarray analysis of human brain samples: the impact of postmortem factors, RNA characteristics, and histopathology, J. Neurosci. Methods 165 (2007) 198–209.
- [71] I.G. Romero, A.A. Pai, J. Tung, Y. Gilad, RNA-seq: impact of RNA degradation on transcript quantification, BMC Biol. 12 (2014) 42.
- [72] C. Bevilacqua, S. Makhzami, J.-C. Helbling, P. Defrenaix, P. Martin, Maintaining RNA integrity in a homogeneous population of mammary epithelial cells isolated by Laser Capture Microdissection, BMC Cell Biol. 11 (2010) 95.
- [73] J.Y. Yee, L.M.G. Limenta, K. Rogers, S.M. Rogers, V.S. Tay, E.J. Lee, Ensuring good quality RNA for quantitative real-time PCR isolated from renal proximal tubular cells using laser capture microdissection, BMC Res. Notes 7 (2014) 62.
- [74] R. Hitzemann, D. Bottomly, P. Darakjian, N. Walter, O. Iancu, R. Searles, B. Wilmot, S. McWeeney, Genes, behavior and next-generation RNA sequencing, Genes Brain Behav. 12 (2013) 1–12.
- [75] A.E. Butler, A.V. Matveyenko, D. Kirakossián, J. Park, T. Gurlo, P.C. Butler, Recovery of high-quality RNA from laser capture microdissected human and rodent pancreas, J. Histotechnol. 39 (2016) 59–65.
- [76] M.J. Chandley, A. Szebeni, K. Szebeni, J.D. Crawford, C.A. Stockmeier,

- G. Turecki, R.M. Kostrzewa, G.A. Ordway, Elevated gene expression of glutamate receptors in noradrenergic neurons from the locus coeruleus in major depression, Int. J. Neuropsychopharmacol. 17 (2014) 1569–1578.
- [77] F. Jenner, G. van Osch, M. Cleary, I. Ribitsch, U. Sauer, R. van Weeren, P. Brama, Laser capture microdissection of murine interzone cells: layer selection and prediction of RNA yield, J. Stem Cell Res. Ther. 4 (2014) 183–188.
- [78] D.R. Boone, M.-A. Micci, I.G. Taglialatela, J.L. Hellmich, H.A. Weisz, M. Bi, D.S. Prough, D.S. DeWitt, H.L. Hellmich, Pathway-focused PCR array profiling of enriched populations of laser capture microdissected hippocampal cells after traumatic brain injury, PLoS One 10 (2015), e0127287.
- [79] N. Mazurek, A.-L. Frisk, J.M. Beekman, A. Hartwig, K. Meyer, Comparison of progestin transcriptional profiles in rat mammary gland using Laser Capture Microdissection and whole tissue-sampling, Exp. Toxicol. Pathol. 65 (2013) 949–960.
- [80] A. Braun, C. Martinez, S. Schmitteckert, R. Röth, F. Lasitschka, B. Niesler, Site-specific gene expression analysis from archived human intestine samples combining laser-capture microdissection and multiplexed color-coded probes, Neuro Gastroenterol. Motil. 30 (2018) e13261.
- [81] L. Bojmar, E. Karlsson, S. Ellegård, H. Olsson, B. Björnsson, O. Hallböök, M. Larsson, O. Stål, P. Sandström, The role of microRNA-200 in progression of human colorectal and breast cancer, PLoS One 8 (2013) e84815.
- [82] V. Gautam, A. Singh, S. Singh, A.K. Sarkar, An efficient LCM-based method for tissue specific expression analysis of genes and miRNAs, Sci. Rep. 6 (2016) 21577
- [83] R.S. Seelan, D.R. Warner, P.M. Mukhopadhyay, S.A. Andres, I.A. Smolenkova, J.L. Wittliff, M.M. Pisano, R.M. Greene, Epigenetic analysis of laser capture microdissected fetal epithelia, Anal. Biochem. 442 (2013) 68–74.
- [84] A. Vogel, V. Venugopalan, Mechanisms of pulsed laser ablation of biological tissues, Chem. Rev. 103 (2003) 577–644.
- [85] C.A. Foster, D. Mechtcheriakova, M.K. Storch, B. Balatoni, L.M. Howard, F. Bornancin, A. Wlachos, J. Sobanov, A. Kinnunen, T. Baumruker, FTY720 rescue therapy in the dark Agouti rat model of experimental autoimmune encephalomyelitis: expression of central nervous system genes and reversal of blood-brain-barrier damage, Brain Pathol. 19 (2009) 254–266.
- [86] X. Zhan, G.C. Jickling, B.P. Ander, B. Stamova, D. Liu, P.F. Kao, M.A. Zelin, L-W. Jin, C. DeCarli, F.R. Sharp, Myelin basic protein associates with AβPP, aβ 1-42, and amyloid plaques in cortex of alzheimer's disease brain, J. Alzheimer's Dis. 44 (2015) 1213–1229.
- [87] K. Wang, F. Donnarumma, S.W. Herke, P.F. Herke, K.K. Murray, Infrared laser ablation sample transfer of tissue DNA for genomic analysis, Anal. Bioanal. Chem. 409 (2017) 4119–4126.
- [88] Y. Liu, A. Beyer, R. Aebersold, On the dependency of cellular protein levels on mRNA abundance, Cell 165 (2016) 535–550.
- [89] M. Wilhelm, J. Schlegl, H. Hahne, A.M. Gholami, M. Lieberenz, M.M. Savitski, E. Ziegler, L. Butzmann, S. Gessulat, H. Marx, Mass-spectrometry-based draft of the human proteome, Nature 509 (2014) 582–587.
- [90] F. Edfors, F. Danielsson, B.M. Hallström, L. Käll, E. Lundberg, F. Pontén, B. Forsström, M. Uhlén, Gene-specific correlation of RNA and protein levels in human cells and tissues, Mol. Syst. Biol. 12 (2016) 883.
- [91] N. Selevsek, C.-Y. Chang, L.C. Gillet, P. Navarro, O.M. Bernhardt, L. Reiter, L-Y. Cheng, O. Vitek, R. Aebersold, Reproducible and consistent quantification of the Saccharomyces cerevisiae proteome by SWATH-MS, Mol. Cell. Proteomics 14 (2015) 739–749.
- [92] M.S. Robles, J. Cox, M. Mann, In-vivo quantitative proteomics reveals a key contribution of post-transcriptional mechanisms to the circadian regulation of liver metabolism, PLoS Genet. 10 (2014), e1004047.
- [93] A. Alli Shaik, S. Wee, R.H.X. Li, Z. Li, T.J. Carney, S. Mathavan, J. Gunaratne, Functional mapping of the zebrafish early embryo proteome and transcriptome, J. Proteome Res. 13 (2014) 5536–5550.
- [94] B. Zhang, J. Wang, X. Wang, J. Zhu, Q. Liu, Z. Shi, M.C. Chambers, L.J. Zimmerman, K.F. Shaddox, S. Kim, Proteogenomic characterization of human colon and rectal cancer, Nature 513 (2014) 382–387.